The British University in Egypt
BUE Scholar

Civil Engineering | Engineering

2021

Potential advantages of basalt FRP bars compared to carbon FRP bars & conventional steel

Yosra El Maghraby
yosra.elmaghraby@bue.edu.eg

Mohamed Nagib Abou-Zeid Prof.
The American University in Cairo AUC, mnagiba@aucegypt.edu

Ezzeldeen Yazeed El Sayed Ahmed Prof
The American University in Cairo AUC, EYSAHMED@AUCEGYPT.EDU

Follow this and additional works at: https://buescholar.bue.edu.eg/civil_eng

 Part of the Civil Engineering Commons, Structural Engineering Commons, and the Structural Materials Commons

Recommended Citation

El Maghraby, Yosra; Abou-Zeid, Mohamed Nagib Prof.; and El Sayed Ahmed, Ezzeldeen Yazeed Prof, "Potential advantages of basalt FRP bars compared to carbon FRP bars & conventional steel" (2021). *Civil Engineering*. 154.
https://buescholar.bue.edu.eg/civil_eng/154

This Article is brought to you for free and open access by the Engineering at BUE Scholar. It has been accepted for inclusion in Civil Engineering by an authorized administrator of BUE Scholar. For more information, please contact bue.scholar@gmail.com.

Potential Advantages of Basalt FRP Bars compared to Carbon FRP Bars & Conventional Steel

Mariam Zaki[a] , Amira Tobaa[a] , Ahmed Shehata[a] , Farid Mohamed[a] , Ramy Khalef[a] , Yomna Hagras[a] , Reem Abou-Ali[a] , Mayer Farag[a] , Athnasious Ghaly[a] , Magdi Madi[a] , Ezzeldin Sayed-Ahmed [a] , Yosra El-Maghraby[b,*] , and Mohamed Abou-Zeid[a]

[a]*The American University in Cairo, AUC Avenue, P.O. Box 74, New Cairo 11835, Cairo, Egypt.*
[b]*The British University in Egypt, Cairo - Suez Desert Road - El Sherouk City 11837, Cairo, Egypt.*

ARTICLE INFO

Article history:
Received
Received in revised form
Accepted

Available online

Keywords:
Basalt
FRP
Concrete
CFRP
BFRP

ABSTRACT

The use of the various types of FRP (Fiber Reinforced Polymers) composites as a reinforcement for concrete structures is in a continuous increase. This is due to the strengthening properties of FRP and its significant resistance to corrosion when compared to conventional steel. In this study an attempt is taken to evaluate the performance of basalt FRP bars compared with carbon FRP bars and conventional steel bars. Specimens of reinforced concrete will be casted to fulfil this comparison. These beams will comprise a common top reinforcement, stirrups spacing, and concrete properties. The difference is in the bottom reinforcement where it was once steel, Carbon FRP, Basalt FRP, and a hybrid of Basalt FRP and steel. These beams were tested for their behavior under a flexural load through a four-point bending test. The remaining specimens were casted as columns with common stirrups spacing, and concrete properties. The behavior of Basalt FRP, Carbon FRP, and steel reinforcement will be tested upon the application of an axial compressive load. The bonding strength between concrete and the different candidate bars is tested through the bond pull-out test. Furthermore, tests will be conducted on the thermal, chemical, and mechanical properties of the individual bars. This study is expected to yield an Evaluation of the main characteristics of the newly developed Basalt FRP bars and an Identification of the key differences and limitations of using BFRP in concrete structures in relation to CRFP and traditional steel reinforcement of concrete structure.

1. Introduction

The successful incorporation of conventional steel as concrete reinforcement has been dominant over the past decades. However, steel corrosion represents a major threat in the construction industry. Therefore, FRP (Fiber Reinforced Polymer) composites used as concrete reinforcement started emerging and proved to be effective. (Inman et al., 2016). In addition to FRP composites being leading icons in their characteristic strength to weight ratio, they also eliminate the structure durability problems and increase its service life. FRP systems exist as composites of a polymer matrix and a fiber. The matrix acts as the media through which the stress is transferred to the fibers. It, also, binds the fibers and adds protection against surface damage. (Vikas and Sudheer, 2017). The fibers embedded in the matrix could be either glass, aramid, carbon, or basalt. Glass, aramid and carbon fibers have been extensively used in several applications where each has its advantages and disadvantages in terms of strength variation, cost, density, …etc. However, basalt FRP has been introduced but little research has been conducted to understand how it complements the advantages of an FRP system at a relatively low cost (Prince, 2009). Basalt is a volcanic igneous rock that is the most abundant rock type in earth's crust. Basaltic materials have a significant high performance in terms of strength, corrosion resistance, temperature range, thermal stability, resistance to acids, resistance to the alkalinity of concrete, and finally their lower cost grants them an added value. The formation of continuous basalt fibers was initiated in 1984 and was found to require less energy, than that required for glass or carbon fibers (Inman et al., 2017). Hence, basalt fibers are environmentally safer than alternative FRP composites. This study attempts to evaluate the performance of basalt FRP (BFRP) bars compared with carbon FRP (CFRP) bars and conventional steel bars (Salh, 2014). Where the Carbon FRP has the advantage of having high strength to weight ratio while its major disadvantage is its high cost. On the other hand, Basalt FRP possesses relatively similar properties with lower cost. Basalt FRP possesses other multiple advantages such as thermal stability, chemical stability, environmentally friendly and economical (Prince, 2009). The major disadvantage of steel is its inability to resist corrosion which eventually leads to structural damages. Fourteen specimens of reinforced concrete were casted to fulfil the objective of this research. Eight of which were beams with common top reinforcement, stirrups spacing, and concrete properties. The difference was in the bottom reinforcement where it varied among steel, CFRP, BFRP, and a hybrid of BFRP and steel. These eight beams were tested for their behavior under flexural load through a four-point bending test. The remaining six specimens were casted as columns with common tie spacing, and concrete properties. The behavior of BFRP, CFRP, and steel reinforcement was tested through the application of an axial load. The bonding strength between concrete and the different bars was tested through the bond pull-out test. Furthermore, tests were conducted to determine the unit weight, tensile strength, water absorption and the thermal and chemical durability of individual bars. The aim of this work is to gain better understanding of the BFRP properties, assess the its potential advantages and disadvantages and determine its cost effectiveness in an attempt to reach a more economic utilization of this fiber which could help designers in making more educated selections when used in concrete works.

2. Objectives and Scope

The objective of this study is to evaluate the potential advantages of BFRP when compared to CFRP and conventional steel. Multiple criteria will be used to perform the evaluation, as it will consider physical, mechanical, structural, chemical, environmental, and economical aspects. Some of these criteria will be met through conducted experimental work, while the remaining will be attained through the literature review.

3. Experimental Program

3.1. *Material Properties*

3.1.1. *Reinforcement Bars*

Table 1: Experimental Properties of Reinforcing Bars

Item	Diameter (mm)	Density (Kg/m³)	Bar Tensile Strength (N/mm²)	Modulus of Elasticity in Tension (N/mm²)
Steel Bar	8,10,12	7636	654	68800
Carbon FRP Bar	12	1600	2900	148000
Basalt FRP Bar	10,12	2348	822	24800

3.1.1.1. Steel Bars

3.1.1.1.1. Columns Reinforcement: 4 longitudinal steel bars with a 12mm diameter (4φ12) and 8mm steel ties every 100mm.

3.1.1.1.2. Beams Reinforcement

- Top reinforcement for all beams: 2 longitudinal steel bars with a 10mm diameter (2φ10).
- Bottom reinforcement for steel reinforced beams: 2 longitudinal steel bars with a 12mm diameter (2φ12).
- Stirrups for all beams: 8 mm steel every 100mm.

3.1.1.2. Carbon FRP Bars

3.1.1.2.1. Columns reinforcement: 4 longitudinal CFRP bars with a 12mm diameter (4φ12) and 8mm steel ties every 100mm.

3.1.1.2.2. Beams reinforcement

- Top reinforcement for all beams: 2 longitudinal steel bars with a 10mm diameter (2φ10).
- Bottom reinforcement for steel reinforced beams: 2 longitudinal CFRP bars with a 12mm diameter (2φ12).
- Stirrups for all beams: 8 mm steel every 100mm.

3.1.1.3. Basalt FRP Bars

3.1.1.3.1. Columns reinforcement: 4 longitudinal BFRP bars with a 12mm diameter (4φ12) and 8mm steel ties every 100mm.

3.1.1.3.2. Beams reinforcement:

- Top reinforcement for all beams: 2 longitudinal steel bars with a 10mm diameter (2φ10).
- Bottom reinforcement for steel reinforced beams: 2 longitudinal BFRP bars with a 12mm diameter (2φ12).
- Stirrups for all beams: 8 mm steel every 100mm.

3.1.2. *Concrete:*

- Fine Aggregates: Normal Sand with a specific gravity 2.6.
- Coarse Aggregates: Well Graded Dolomite (MNA 38 mm) with a specific gravity of 2.8.
- Water: ordinary tap water used in concrete mix and curing.
- Admixture: Superplasticizer to improve concrete workability.
- Cement: Type I Ordinary Portland cement
- Compressive Strength 45 (+/-) 5 N/mm²

The concrete mix with design strength used for all casted specimens was assumed to have an incidental air content of 2% and a water-to-cement ratio of 0.35, a superplasticizer was added to improve the workability at 0.75% by weight of cement content. Table 2 shows the content proportions of the concrete mix design.

Table 2. Concrete mix design

Item	Value
Cement	450 kg/m³
Water	157.5 kg/m³
Fine Aggregates	659 kg/m³
Coarse Aggregates	1186 kg/m³
Slump	70 mm
w/c ratio	0.35
Compressive strength (at 28 days)	45 (+/-) 5 MPa

3.2. *Tests*

3.2.1. *Tests on Fresh Concrete:* slump test was conducted to determine the workability of the poured mix.

3.2.2. *Test on Hardened Concrete:* 7-day compressive strength and 28-day compressive strength tests were conducted each on 3 cubes respectively. The dimensions of the compressive strength cubes were (0.15 m x 0.15 m x 0.15 m).

3.2.3. *Tests on Individual Reinforcement Bars*

3.2.3.1. *Unit Weight Test:* The volume of individual bars and their corresponding weights were measured to obtain the unit weight of the bar according to ASTM C138. This was performed on 3 specimens from each candidate reinforcement with a 12 mm diameter.

3.2.3.2. *Water Absorption Tests:* According to ASTM D570 the bar was weighed then immersed in water for 24 hours, surface dried then re-weighed to obtain the amount of water it absorbed. This was performed on 3 specimens from each candidate reinforcement of length 20 cm and diameter of 12 mm.

3.2.3.3. *Chemical Durability (Alkali Resistance) Test:* According to ASTM E 2098-00, the initial weight and volume of the specimens were recorded, then the specimens were exposed to 1 M concentration of NaOH solution for 14 days, then their weight and volume were re-measured after their exposure and any changes were recorded. This was performed on 3 specimens from each candidate reinforcement of length 3 cm and diameter of 12 mm.

3.2.3.4. *Chemical Durability (Acidic Resistance) Test:* The initial weight and volume of the specimens were recorded, then the specimens were exposed to 1 M concentration of H_2SO_4 solution for 14 days. Then their weight and volume were re-measured after their exposure and any changes were recorded. This was performed on 3 specimens from each candidate reinforcement of length 3 cm and diameter 12 mm. This test was deduced from the standard acidity test.

3.2.3.5. *Thermal Stability Test:* The bars were placed in an oven at a temperature of 100°C for 2 hours, then their tensile strength was measured (according to ASTM A370/ D7205) and compared with tensile strength properties before heating. This is performed on 2 specimens from each candidate reinforcement of gauge length of 12 cm and a diameter of 12 mm

3.2.4. *Tests on Hardened Concrete Reinforced with candidate bars*

3.2.4.1. *Bond Pull-out Test:* a total of 6 cylinders of concrete reinforced with one central bar (2 of each candidate reinforcement) are casted of a 30 cm height and 15cm diameter. The bar protruded from one side of the cylinder in order to be pulled out with an embedded length equal to the height of the cylinder (30 cm). In addition to that, the FRP bars were embedded in a steel casing through an epoxy mortar in order to prevent slippage from the grip of the pulling machine. The strain rate applied by the MTS machine was 0.2 mm/min.

3.2.4.2. *Test on Beams:* a total of eight beams were tested with the main objective of comparing the BFRP and CFRP reinforced beams with the concrete beams reinforced with conventional steel bars with regard to strength, ductility, and deflection. The eight beams include two CFRP

reinforced beams, two BFRP reinforced beams, two steel reinforced beams, and two hybrid beams. The hybrid beam configuration consisted of a bottom reinforcement of one bar of steel and one bar of BFRP. All the bars in the bottom reinforcement were of a 12 mm diameter, the remaining parameters were kept constant in order to allow for a valid comparison. The parameters that were kept constant include the top reinforcement of the beams which consisted of 2 steel bars of a 10 mm diameter, the stirrups which consisted of steel of 8 mm diameter at a spacing of 100 mm along the beam, the reinforcement ratio “0.017”, the concrete used which followed the mix design described in Table 2, and the beam dimensions which were (0.15 m x 0.15 m x 1 m). The beams were subjected to a four-point bending test at a testing span of 0.8 m between the 2 supports. In addition to that, strain gauges were attached to measure the strain in the bottom reinforcing bars. As shown in Figure 1, the position of the strain gauge is marked with the blue star. Four beam configurations were developed and their cross section demonstrated in Figure 1.

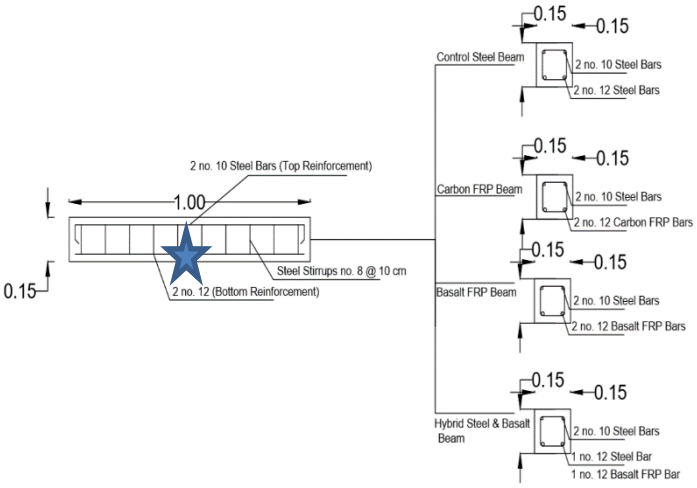

Figure 1 Configuration of Beam Reinforcement

(Figure for test setup with dimensions needed, can add dimensions to fig 7 and refer to it

3.2.4.3. *Test on Columns:* a total of 6 columns were tested to observe the behavior of columns reinforced with BFRP bars and CFRP bars in comparison to conventional steel reinforced columns. The columns were divided in to 2 categories, first of which is the 12 mm diameter category and the second is the 10 mm diameter category. Each category had a control column which was steel reinforced. The 12 mm category consisted of 2 (12 mm diameter) CFRP reinforced columns, while the 10 mm category consisted of 2 (10 mm diameter) BFRP reinforced columns. All columns had the same dimensions which were (0.75 m x 0.15 m x 0.15 m). The same reinforcement ratio was used in all columns (4 reinforcement bars), in addition to that the stirrups which consisted of steel of 8 mm diameter at a spacing of 100 mm along the column. This dense confinement provided by the stirrups is used as safety measure taken for the columns to reduce the catastrophic failure of the columns reinforced with the FRP material as their predicted mode of failure is brittle. Further confinement was added through U-shaped stirrups that form a column top and bottom cap to reduce the stresses that might cause failure at these points and create misleading results. Moreover, strain gauges were attached to the bars at the bottom 1/3 of the column height to measure the strain in the bars at the critical region under the compressive load. As shown in Figure 2, the position of the strain gauges is marked with the blue star. Four Column configurations were developed and their cross section demonstrated in Figure 2.

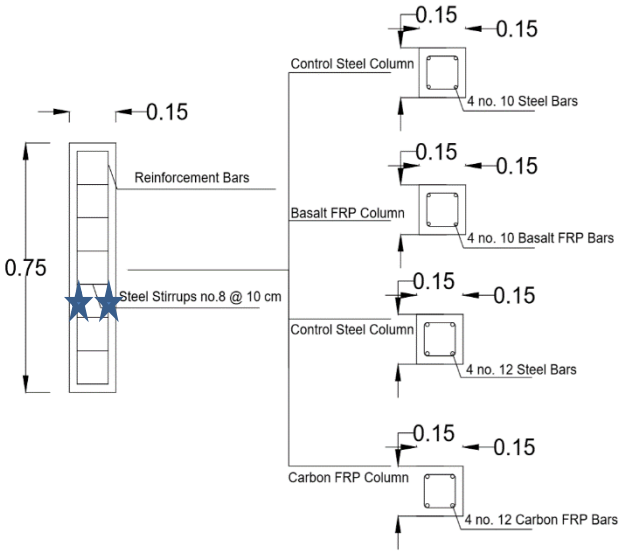

Figure 2 Configuration of Column Reinforcement

4. Results and Discussions

Results of Individual Reinforcement Bar Tests

4.1.1. *Unit Weight:* Unit weight tests were conducted on basalt, carbon, and steel rods. Basalt and Carbon FRP rods unit weights were comparable. The Basalt rod recorded a value of 2348 kg/m3, and the Carbon rod recorded a value of 1842 kg/m3. On the other hand, the steel recorded a value three to four times the value of the FRPs, it had a unit weight of 7636 kg/m3.

4.1.2. *Water Absorption:* The specimens proved to be impermeable to water as they showed stability in weight and volume upon the 24 hours in water.

4.1.3. *Chemical Durability (Alkali Resistance):* All the three specimens showed no change in their physical properties or their appearance. There was no degradation in their surfaces, and they neither lost weight nor volume. This test can prove that the three specimens can sustain the alkalinity of the cement inside the concrete.

4.1.4. *Chemical Durability (Acidity Resistance):* The CFRP and BFRP have not experienced any change in their physical properties and this was proven by their stability in weight and volume. However, the steel specimen has been affected by the acid, as seen in Figure 3, through surface degradation, corrosion, and hence loss in weight.

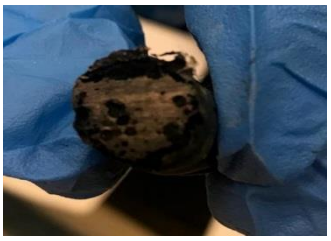

Figure 3. Surface degradation of steel specimen

4.1.5. *Thermal Stability*

4.1.5.1. *Initial Attempt (keeping bars at 600°C for 2 hours):* This temperature was selected as a representable one according to the literature review which indicated that all three candidate bars can maintain their properties up to 800°C, which after experimentation the CFRP bars proved to disintegrate completely from the matrix as shown in Figure 4. While the epoxy in the BFRP bars’ matrix expanded leaving air voids inside the bar and making it more brittle. No physical damage occurred to the steel bars (Figure 5).

Figure 4. CFRP bars after 2 hours at 600°C

Figure 5 BFRP before (left) and after (right) heating.

4.1.5.2. *Modified Attempt (keeping bars at 100°C for 2 hours):* This temperature was selected upon checking the thermal stability technically specified by the suppliers of the bars, where the BFRP bars were designed to sustain their properties up to 300°C, while the CFRP bars were designed to sustain their properties up to 150°C. Therefore, a temperature of 100°C was chosen to be representable as to determine whether the bars lose strength upon exposure to high temperature. After being kept at 100°C for 2 hours and then left to cool for an appropriate time. All three bars exhibited no change in their physical properties as shown in Figure 6. Then the tensile strength test was conducted upon them where the steel bar was found to lose 6% of its ultimate tensile strength while the BFRP lost 10%. The CFRP specimens failed during testing due to slippage within the material.

Figure 6 Steel, CFRP, BFRP (left to right) after heating

Table 3 Temperature effect on bar tensile strength

Bar Type	Normal tensile strength(N/mm2)	Reduced tensile strength(N/mm2)	Loss In tensile Strength (%)
Steel bar	654	609	6
CFRP bar	-	-	-
BFRP bar	822	737	10

4.2. *Results of Hardened Concrete Tests*

4.2.1. *Bond Test Results:* The steel specimen showed a ductile failure in the bar at 70 KN. Figure 7 shows the results of the CFRP cylinder.

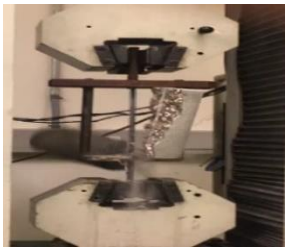

Figure 7 CFRP reinforced cylinder

Figure 8 BFRP reinforced cylinder

There was a crack along the centerline of the cylinder where failure occurred at 87 kN. Finally, the BFRP showed a crack along the center line (Figure 8), however, it did not fail along it, rather it failed due to a crack in the upper third of the cylinder that initiated due to a weak point that was created because of excess water or concrete bleeding (a phenomenon that occurs in concrete incase coarse aggregates settle in the bottom resulting in the rise of free water to the surface). It failed at 74.5 KN. Although according to literature, it was expected to fail at the same load as the carbon specimen if it did not fail due to the weak point mentioned earlier. Apparently, the bond between the BFRP bar & the concrete was stronger than the weak point where failure occurred. Table 4 shows a comparison between the failure loads of the 3 specimens due to the bond test.

Table 4 Bond Test Results

Specimen	Mode of Failure	Failure Load
Steel	Ductile failure in steel bar	70 kN
CFRP	Cylinder split in half	87 kN
BFRP	Crack along centerline but failure due to a crack in the top third	74.5 kN

4.2.2. *Test Results on Beams*

The prepared beams were tested using a four-point loading bending test as described in the experimental program section. This particular setup was chosen in order to create a region of zero shear and a constant maximum moment in the beams (Fareed et al., 2016). As seen in Figure 9, cracks initiated in the constant moment region then stretched towards the supports and this was a general behavior for all the specimens. In addition to that, a horizontal crack formed at the top of the beam between the 2 loading points.

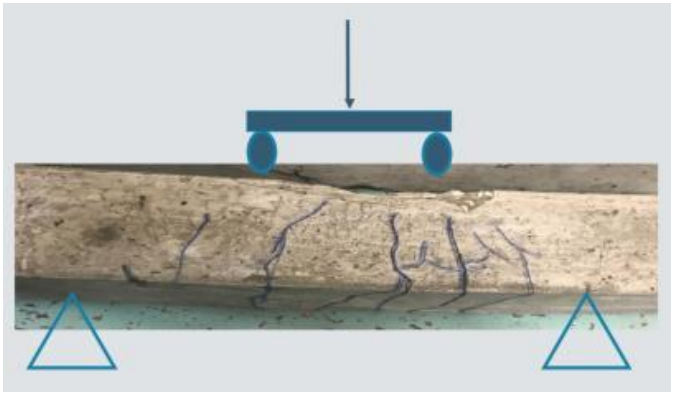

Figure 9 Beam reinforced with steel after testing

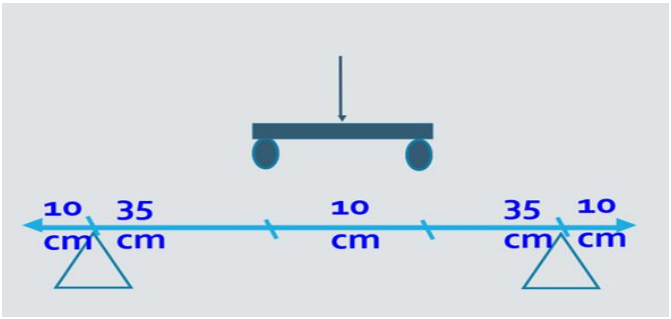

Figure 10 Configuration of the Four Point Bending Test

4.2.2.1. *Steel Reinforced Beams:* This beam carried an ultimate load of 107 kN. By using the Whitney stress block (Figure 11) this beam was estimated to carry an ultimate load of 81.9 kN. The Whitney Stress Block estimates a theoretical ultimate load expected to be carried by the section of a beam.

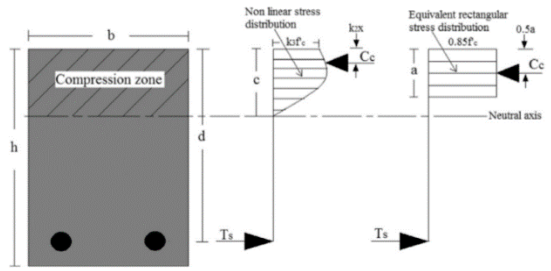

Figure 11 Whitney Stress Block

This minor discrepancy is due to factors of safety included and theoretical variable implied in the equations. The load vs deformation at mid-span of the beam curve (Figure 12) was obtained in addition to the load vs strain curve obtained from the attached strain gauges was also developed (Figure 13) from which the energy absorbed by the beam and the ductility index (Equation 1) was calculated to indicate the ductility of the steel beam to be compared with the remaining specimens.

$$Ductility\ Index = \frac{Deformation\ at\ ultimate\ load}{Deformation\ at\ yield\ load} (1)$$

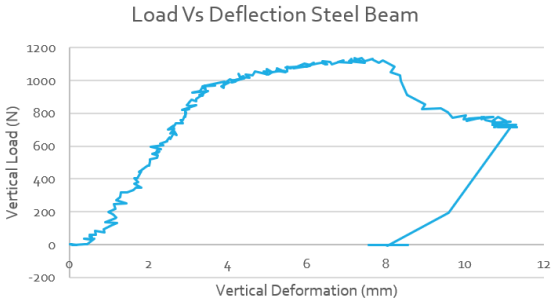

Figure 12 Load Vs. Deflection Steel Beam

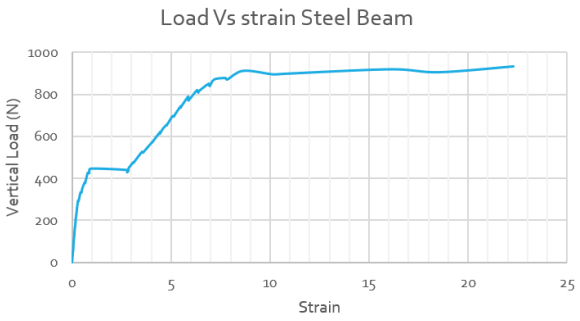

Figure 13 Load Vs. Strain Steel Beam

Table 5 Steel Beam Ductility Parameters

Energy Absorbed by Beam	0.913 kN.m	Ductility Index	4.12

4.2.2.2. *CFRP Reinforced Beams:* This beam carried an ultimate load of 129 kN, while it was theoretically expected to carry 206 kN. Such extreme discrepancy occurred due to two concrete cracks enclosing a very large deformation of CFRP bars. Occurrence of such deformation resulted in high stresses at the interface between the concrete and the CFRP bars leading the system to release the stress by slippage of the CFRP bars from the concrete. This slippage occurred due to the interface between the CFRP bars and the concrete being the weakest point in the system rather than the concrete itself or the CFRP bars. The load vs deflection at mid-span of the beam curve (Figure 14) was obtained in addition to the load vs strain curve (Figure 15) obtained from the attached strain gauges was also developed from which the energy absorbed by the beam and the ductility index were calculated (Table 6) to indicate the ductility of the CFRP beam to be compared with the remaining specimens.

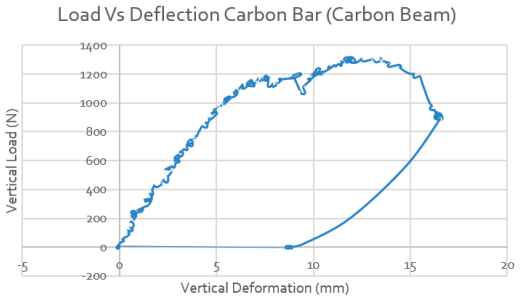

Figure 14 Load Vs. Deflection Carbon FRP Beam

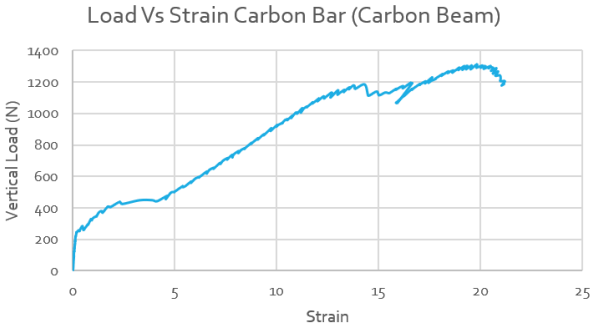

Figure 15 Load Vs Strain Carbon FRP Beam

Table 6 Carbon FRP Beam Ductility Parameters

Energy Absorbed by Beam	1.69 kN.m	Ductility Index	5.4

4.2.2.3. *BFRP Reinforced Beams:* This beam carried an ultimate load of 95 kN, while it was theoretically expected to carry 145 kN. This discrepancy is smaller than that of the CFRP reinforced beam, due to minimal slippage in the bars due to the sand coating on the BFRP bars that improves their bond with concrete. The load vs deflection at mid-span of the beam curve was obtained (Figure 16) in addition to the load vs strain curve (Figure 17) obtained from the attached strain gauges was also developed from which the energy absorbed by the beam and the ductility index were calculated (Table 7) to indicate the ductility of the BFRP beam to be compared with the remaining specimens.

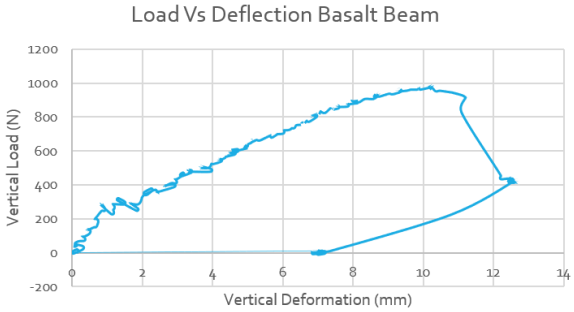

Figure 16 Load Vs. Deflection Basalt FRP Beam

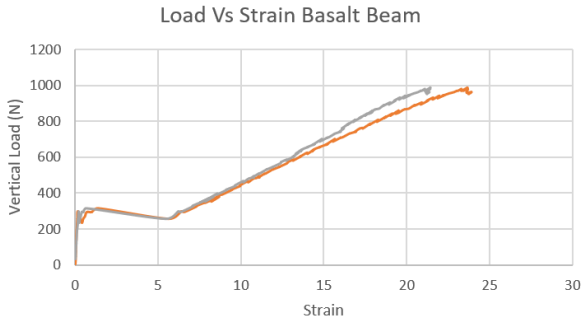

Figure 12 Load Vs. Strain Basalt FRP Beam

Table 7 Basalt FRP Beam Ductility Parameters

Energy Absorbed by Beam	0.64 kN.m	Ductility Index	3.3

4.2.2.4. *Hybrid Beam:* The hybrid beam solution was proposed to enhance the ductility of the BFRP beam, as it alone had the least ductility index and energy absorbed by the beam which both indicated the low ductility of the BFRP beam. The load vs deformation at mid-span of the beam curve (Figure 18) was obtained in addition to the load vs. strain curve (Figure 19) obtained from the attached strain gauges was also developed from which the energy absorbed by the beam and the ductility index were calculated (Table 8) to indicate the ductility of the hybrid beam to be compared with the remaining specimens. The beam carried an ultimate load of 112 kN, while the theoretically calculated was 119.5 kN.

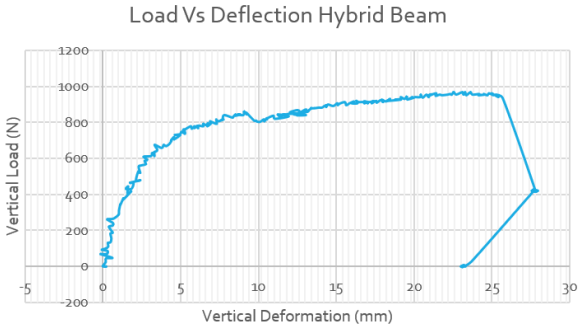

Figure 13 Load Vs. Deformation Hybrid Beam

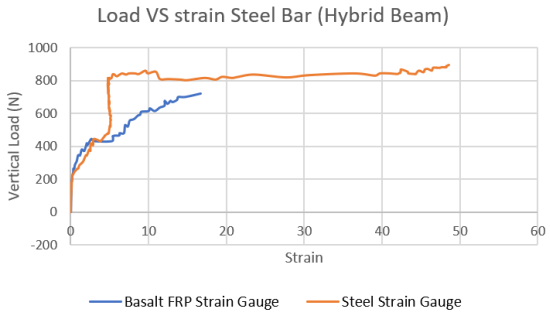

Figure 14 Load Vs. Strain Hybrid Beam

Table 8 Hybrid Beam Ductility Parameters

Energy Absorbed by Beam	1.98 kN.m	Ductility Index	5.4

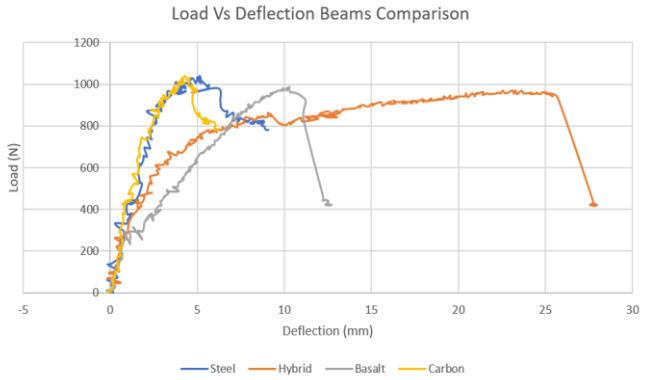

Figure 20 Comparison of Load Vs. deformation curves of all beams

Table 9 Comparison of Ductility Parameters

Beams	Steel	CFRP	BFRP	Hybrid
Energy Absorbed (kN.m)	0.913	1.69	0.64	1.98
Ductility Index	4.12	5.4	3.3	5.4

The Energy absorbed was calculated by using the Load vs. Deflection at midspan of the beam. Then the deflection at midspan is multiplied by the load applied to obtain the energy absorbed by the beam to undergo such deflection (Area under the curve). The main parameter used to compare the beam was their ductility through ductility index and energy absorbed. Ductility Index was calculated using (Equation 1) where the deformation at yield load is obtained through drawing a tangent on the load vs. strain Graph at the ultimate load and another one at the point where the elastic region has just ended. These tangents are to be extrapolated until intersection, then a vertical line drawn from their intersection until it intersects the graph again. The load at the second intersection point (with the graph) is the theoretical yield load, then this load is allocated back into the load Vs. Deflection Graph to obtain the deflection at midspan upon which such load was applied.

4.2.3. *Test Results on Columns*

4.2.3.1. *12mm Diameter Category:* The strain was obtained from the load vs strain curve and the energy absorbed by the columns was calculated from the area under the load vs deformation curve. On the other hand, a much higher strain in the CFRP bars was created at the same load. After the cracking of the concrete occurred, the CFRP bars kept carrying part of the stress, therefore a higher strain was generated. The energy absorbed by the CFRP column was less than that of the steel column and this was shown by the drastic failure which was extremely catastrophic as the column failed suddenly by bursting out.

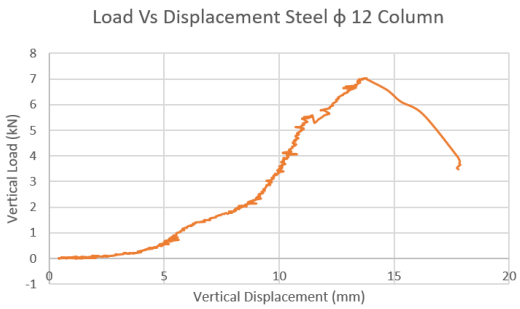

Figure 21 Load Vs Deformation Steel ϕ12 Column

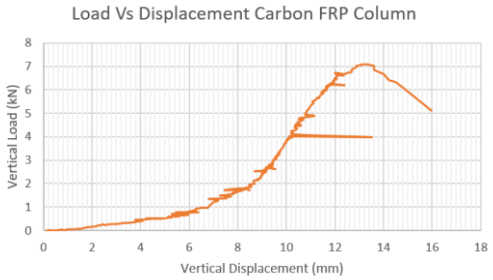

Figure 22 Load Vs Deformation Carbon FRP Column

4.2.3.2. *10mm Diameter Category:* The second steel control column was compared to the BFRP column where reinforcement for both bars was 10 mm diameter. The BFRP column carried an ultimate load 7% higher than the steel column. The energy absorbed by the BFRP column was three times higher than the steel column indicating that modes of failure were visible without suddenly failing. Table 4 indicates a comparison of the columns test results.

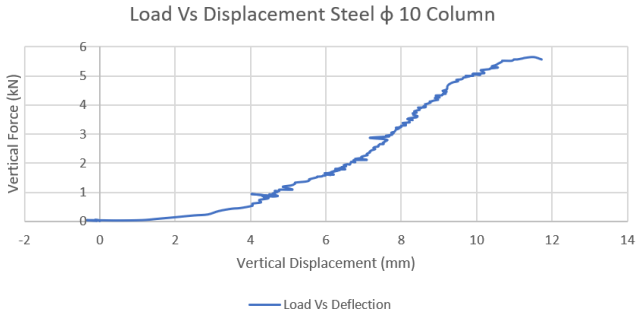

Figure 23 Load Vs Deformation Steel ϕ10 Column

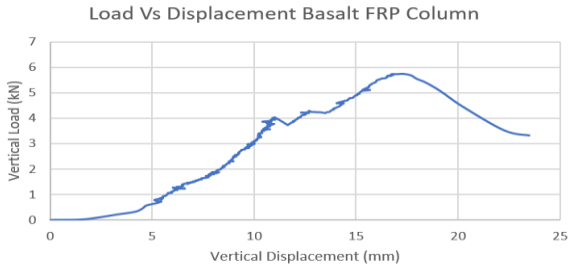

Figure 24 Load Vs Deformation Basalt FRP Column

Table 10 Columns Results Comparison

Column Reinforcement	Ultimate load (kN)	Strain in bars at ultimate load	Energy absorbed by column (kN.mm)
Steel (φ12)	690	1453	4.92
CFRP (φ12)	660	2162	4.36
Steel (φ10)	550	2050	2.64
BFRP (φ10)	590	1888	7.31

5. Conclusions

- Both Basalt & Carbon FRP bars can carry ultimate stresses higher than steel conjugate bars but with significant reduction in ductility.
- FRP bars both from basalt & carbon have good resistance to temperature at least up to 100 °C.
- The hybrid section gave the highest ductility compared to all other sections tested indicated by the energy absorbed by the section upon deformation.
- In both applications, beams & columns, BFRP bars performed considerably well when compared to other reinforcement bars, which invites their use in the reinforced concrete industry.
- FRP bars have a higher market initial cost when compared to steel, yet such increase is expected to diminish gradually upon wider use keeping in mind, other unique advantages such as corrosion resistance which reduces its life-cycle cost according to the case study by Mackechnie and Alexander in 2001 (Mackechnie and Alexander, 2001).
- FRP bars, both Basalt and Carbon possess superior resistance to acids and alkalis

6. Recommendations

- Expand this work on much larger specimens and concrete mixes for longer durations to validate the findings.
- To reduce errors in values of results of the tensile test on the individual bars, attach strain gauges to rather measure their own strain.
- Increase the number of strain gauges used on bars in columns & beams in case a technical error causes the gauges to stop working
- To further understand thermal stability of candidate bars, measure their tensile strength at increments of temperatures to establish a relationship between temperature exposure and loss in mechanical properties
- Test the durability of bars upon exposure to harsher environments at elevated temperatures
- In the reinforced concrete applications of the candidate bars use high strength concrete to explore different failure modes
- Consider the use of Basalt FRP bar as well as Carbon FRP bars in structures subjected to corrosion and chemical attack
- Apply an epoxy coat on Carbon FRP bars while using them as a reinforcement for concrete.
- Suggest a hybrid system at early implementation of Basalt FRP bars to capitalize on its high ductility properties
- Promote the manufacturing and production of basalt fibers in order to contribute to minimizing its cost
- It is aspired for such new material to be covered in a newer version in the Egyptian code to facilitate its wider use.

References and notes

1. Marianne Inman, Eythor Rafn Thorhallsson and Kamal Azraguea. A Mechanical and Environmental Assessment and Comparison of Basalt Fibre Reinforced Polymer (BFRP) Rebar and Steel Rebar in Concrete Beams 111 pp 31-40, 2017.
2. Vikas G. and Sudheer M., American Journal of Materials Science 2017, 7(5): 156-165 DOI: 10.5923/j.materials.20170705.07
3. Richard E. Prince. Fibre Reinforced Polymers Characteristics and Behaviors, Prince Lund Engineering 2009, https://www.princelund.com/fiber-reinforced-polymers.html

4. JR Mackechnie, and MG Alexander. Repair Principles for Corrosion-damaged Reinforced Concrete Structures. Publication no. 5. Department of Civil Engineering, University of Cape Town. 2001.
5. Luna Salh. Analysis and Behaviour of Structural Concrete Reinforced with Sustainable Materials. Report. School of Engineering, University of Liverpool. University of Liverpool, 2014.
6. ASTM D7205, Standard Test Method for Tensile Properties of Fiber Reinforced Polymer Matrix Composite Bars 2016, www.astm.org.
7. Fareed Elgabbas, Vincent Patrick, Ehab Ahmed, and Brahim Benmokrane. Experimental Testing of Basalt- fiber-reinforced Polymer Bars in Concrete Beams. Composites Part B: Engineering 91, pp 205-218, 2016.